

Consequences of neutrino self-interactions for weak decoupling and big bang nucleosynthesis

To cite this article: E. Grohs et al JCAP07(2020)001

View the article online for updates and enhancements.



IOP ebooks™

Bringing together innovative digital publishing with leading authors from the global scientific community.

Start exploring the collection-download the first chapter of every title for free.

Consequences of neutrino self-interactions for weak decoupling and big bang nucleosynthesis

E. Grohs, a,1 George M. Fuller and Manibrata Sena,c

^aDepartment of Physics, University of California, Berkeley, 366 LeConte Hall, Berkeley, California 94720, U.S.A.

E-mail: egrohs@berkeley.edu, gfuller@ucsd.edu, manibrata.sen@gmail.com

Received February 27, 2020 Revised April 18, 2020 Accepted May 5, 2020 Published July 1, 2020

Abstract. We calculate and discuss the implications of neutrino self-interactions for the physics of weak decoupling and big bang nucleosynthesis (BBN) in the early universe. In such neutrino-sector extensions of the standard model, neutrinos may not free-stream, yet can stay thermally coupled to one another. Nevertheless, the neutrinos exchange energy and entropy with the photon, electron-positron, and baryon component of the early universe only through the ordinary weak interaction. We examine the effects of neutrino self-interaction for the primordial helium and deuterium abundances and $N_{\rm eff}$, a measure of relativistic energy density at photon decoupling. These quantities are determined in, or may be influenced by, the physics in the weak decoupling epoch. Self-interacting neutrinos have been invoked to address a number of anomalies, including as a possible means of ameliorating tension in the Hubble parameter. Our calculations show that surprisingly subtle changes in BBN accompany some of these neutrino self-interaction schemes. Such minute signals require high-precision measurements, making deuterium the best abundance for BBN constraints in the models explored here.

Keywords: big bang nucleosynthesis, cosmological parameters from CMBR, cosmological neutrinos

ArXiv ePrint: 2002.08557

¹Corresponding author.

^bDepartment of Physics, University of California, San Diego, 9500 Gilman Drive, La Jolla, California 92093-0319, U.S.A.

^cDepartment of Physics and Astronomy, Northwestern University, 2145 Sheridan Road, Evanston, Illinois 60208-3112, U.S.A.

1	Int	roduction	1
2	Overview of Big Bang Nucleosynthesis		4
	2.1	Physics	4
	2.2	Numerics	5
		2.2.1 Computational code	7
		2.2.2 Results in the standard scenario	7
3	Lep	oton symmetric initial conditions	7
	3.1	Neutrino transport with self-interactions	7
	3.2	Results	9
		3.2.1 Neutrino spectra	9
		3.2.2 Primordial abundances	12
4	Dai	12	
	4.1	Dark radiation parameter	12
	4.2	Results	12
		4.2.1 Neutrino spectra	12
		4.2.2 Primordial abundances	13
5	Lep	oton asymmetric initial conditions	14
	5.1	Differences in implementation with symmetric scenario	14
	5.2	Results	15
		5.2.1 Neutrino spectra	15
		5.2.2 Primordial abundances	16
6	Coı	17	
	6.1	Summary	17
	6.2	Discussion	18

1 Introduction

Contents

In this paper we report detailed calculations of the evolution of the early universe when self-interacting neutrino standard model extensions are adopted. Though many properties of the neutrinos have been measured, including the mass-squared differences and three of the four parameters in the unitary transformation between the neutrino weak interaction (flavor) basis and the mass basis [1], much remains unexplored and mysterious in this sector of particle physics. Indeed, many extensions of the standard model in the neutrino sector have been proposed, and for a variety of purposes. Standard model extensions that posit interactions among the neutrinos only — sometimes termed self-interactions or "secret" interactions — are notoriously difficult to constrain in experiments. However, two astrophysical venues perhaps offer a window into this physics. Both the early universe [2] and collapsing or merging compact objects [3] at some point have their energy and dynamics influenced by neutrino-neutrino scattering. The former venue is a promising test bed for this physics because of

the advent of high precision cosmology; the latter because of the burgeoning capabilities in multi-messenger astronomy. Cosmological invocations of Self-Interacting Neutrino (SI ν) models include attempts to: reconcile sterile neutrino interpretations of neutrino anomalies with cosmological bounds [4–7]; produce sterile-neutrino dark matter [8, 9]; suppress active neutrino free-streaming [2]; and act as a principal participant in schemes crafted to reconcile discordant measurements of the Hubble parameter [10, 11]. SI ν can also put constraints on models of inflation [12, 13] and influence flavor evolution of dense neutrino streams in compact objects [14–16].

There are many standard model extensions in the neutrino sector which incorporate neutrino self-interactions. Some of these, for example, singlet Majoron and Familon models [17–19] envision a spontaneously broken symmetry with a Goldstone boson which mediates neutrino self-interactions. In these models, exchange of this boson engenders flavor-changing interactions among the neutrinos with interaction strengths that can be many orders of magnitude stronger than the standard model weak interaction. Here we consider a scalar-exchange model based off of eq. (2) in ref. [9]. The interaction Lagrangian \mathcal{L}_{int} has effective couplings G_{ij} between neutrino species i and j

$$\mathcal{L}_{\text{int}} = g_{ij} \overline{\nu_{iL}^c} \nu_{jL} \varphi + g_{ij} \overline{\nu_{iL}} \nu_{jL}^c \varphi^*, \quad G_{ij} = \frac{g_{ij}^2}{m_{\varphi}^2}, \tag{1.1}$$

where ν_L is a left-handed-neutrino Dirac spinor and m_{φ} is the rest mass of the scalar exchange particle φ . The superscript c on the Dirac spinor indicates charge conjugation. With the model in eq. (1.1), neutrinos cannot undergo spin-flips at order g^2 . Spin-flips are possible at order g^3 , but such a mechanism requires other features of an ultraviolet-complete theory, e.g., eq. (1.3) in ref. [20]. The overall coupling G_{ij} is analogous to the Fermi constant G_F in the standard weak interaction, so that typical cross sections in our adopted schematic self-interaction model will scale with energy as $\sigma_{ij} \sim G_{ij}^2 E_{\nu}^2$. References [20, 21] study how to embed the operator in eq. (1.1) into UV-complete models.

In this work we will consider only processes which couple neutrinos to other neutrinos, albeit with flavor changing currents. Specifically, we include $\nu\nu$ and $\overline{\nu}\overline{\nu}$ s-channel processes and $\nu\overline{\nu}$ t-channel processes, where the later manifests in lepton-asymmetric systems. We will not consider processes which convert a neutrino into an anti-neutrino. It is most convenient to represent the couplings in our generic model in flavor-basis matrix form:

$$[g_{ij}] = \begin{pmatrix} g_{ee} & g_{e\mu} & g_{e\tau} \\ g_{\mu e} & g_{\mu\mu} & g_{\mu\tau} \\ g_{\tau e} & g_{\tau\mu} & g_{\tau\tau} \end{pmatrix} \Rightarrow g \begin{pmatrix} 1 & 1 & 1 \\ 1 & 1 & 1 \\ 1 & 1 & 1 \end{pmatrix}.$$
(1.2)

Here the flavor off-diagonal entries produce flavor-changing couplings. The second matrix represents the coupling scheme we adopt for our early universe weak decoupling and Big Bang Nucleosynthesis (BBN) calculations. We employ an overall coupling strength g and equal strength in all neutrino-neutrino scattering channels, including those which change flavor. Our generic model then has two independently specifiable quantities: g and m_{φ} .

We will further restrict the range of neutrino self-interaction parameters we actually simulate by restricting the mass of the scalar m_{φ} to be much larger than the range of temperatures T that our weak decoupling neutrino transport and nuclear reaction calculations cover. In other words, we will assume $m_{\varphi} \gg T$. The temperature range of our calculations span the entire weak decoupling and BBN epoch. Generously, and therefore conservatively, we

take this range to be $30\,\mathrm{MeV} > T > 1\,\mathrm{keV}$. Restricting the scalar mass to be $m_\varphi \gg 30\,\mathrm{MeV}$ means that we will not have to be concerned with on-shell production and population of these particles during weak decoupling. Moreover, though the scalar particles may be produced in significant abundance early on, for example at temperatures $T > m_\varphi$, we will consider only coupling strengths g sufficiently large to keep these particles in equilibrium with the neutrino component. This guarantees that the scalar particles will have disappeared by the beginning time of our simulations. Such relatively large couplings also preclude out-of-equilibrium scalar particle decays and concomitant entropy generation during weak decoupling and BBN. We note, however, that cosmology does not provide the only constraint on SI ν models [22].

Finally, we assume that the overall coupling g is large enough to produce efficient energy and flavor exchange among the neutrinos. We compare the self-interacting neutrino scattering rate, $\Gamma_{\rm SI}$, to the Hubble expansion rate, H, to estimate when the neutrinos decouple from themselves

$$\Gamma_{\rm SI} \sim H \implies \left(\frac{g^2}{m_{\varphi}^2}\right)^2 \langle E^2 \rangle n_{\nu} \sim \sqrt{\frac{8\pi}{3}} \frac{\pi^2}{30} g_{\star} \frac{T^2}{m_{\rm pl}},$$
(1.3)

where $\langle E^2 \rangle$ is the average square energy, n_{ν} is the number density of neutrinos, g_{\star} is the relativistic degrees of freedom [23], and $m_{\rm pl}$ is the Planck mass. If we approximate $\langle E^2 \rangle \approx T^2$ and use Fermi-Dirac (FD) statistics for 3 flavors of neutrinos to deduce $n_{\nu} = 3 \times 3\zeta(3)T^3/(4\pi^2)$, we can solve for g

$$g \sim 5.2 \times 10^{-2} \left(\frac{m_{\varphi}}{30 \,\text{MeV}}\right) \left(\frac{1 \,\text{keV}}{T}\right)^{3/4} \left(\frac{g_{\star}}{3.36}\right)^{1/8}.$$
 (1.4)

For a decoupling temperature $T \simeq 1 \,\mathrm{keV}$, we estimate an effective coupling $G_{\mathrm{eff}} \equiv g^2/m_{\varphi}^2 \simeq 3.0 \times 10^{-6} \,\mathrm{MeV^{-2}}$, in line with the models proposed in ref. [11] to alleviate the Hubble parameter tension [24]. For $m_{\varphi} = 30 \,\mathrm{MeV}$, kaon decay [25, 26] rules out a universal coupling in this range [22], implying the mediator mass must be larger than $\sim 100 \,\mathrm{MeV}$. With our assumption that $m_{\varphi} \gg T$, this "self-equilibrium" in the neutrino component is effected via two-to-two neutrino scattering processes on timescales short compared to standard charged-and neutral-current weak interaction times, and for the entire temperature range employed in our calculations.

The neutrino component will be essentially instantaneously self-coupled and energy-and flavor-equilibrated in this model. However, the neutrinos will exchange energy and entropy with the photon-electron-positron-baryon plasma only through the ordinary standard model weak interactions. This sets up a formidable transport problem wherein we must follow self-consistently the flow of energy and entropy between the various components while simultaneously calculating the strong, electromagnetic and weak interactions that determine the quantities that can be probed, i.e., the light element abundances and relic neutrino energy density. The latter quantity derives from the inferred radiation energy density $\rho_{\rm rad}$ at the photon decoupling epoch, $T \approx 0.2\,{\rm eV}$, and is parameterized by $N_{\rm eff}$, defined through

$$\rho_{\rm rad} = \left[2 + \frac{7}{4} \left(\frac{4}{11} \right)^{4/3} N_{\rm eff} \right] \frac{\pi^2}{30} T^4. \tag{1.5}$$

The outline of this paper is as follows. To describe the $SI\nu$ scenario, it will prove helpful to give a brief review of BBN in section 2. Subsections 2.1 and 2.2 describes the physics and numerics of BBN with particular emphasis on the evolution of the neutrino

seas. In section 3, we present our first $SI\nu$ results with neutrino-anti-neutrino symmetric initial conditions. Subsection 3.1 specifies the physics and computational model of $SI\nu$, and subsection 3.2 gives results. To further investigate self-interactions during BBN, we provide two extensions to standard BBN with an addition of dark radiation and neutrino-anti-neutrino asymmetric initial conditions in sections 4 and 5. We summarize our results and discuss further implications of self-interacting neutrinos in section 6. Throughout this paper we set $c = \hbar = k_B = 1$.

2 Overview of Big Bang Nucleosynthesis

We direct the reader to refs. [23, 27–29] for a treatment on the basic physics of BBN, and ref. [30] for an overview of the current status of the field. We give a brief review on the relevant topics of standard BBN here to contrast the standard scenario with that of $SI\nu$.

2.1 Physics

Big Bang Nucleosynthesis is a succession of out-of-equilibrium freeze-outs. The first freeze-out epoch is weak decoupling, when the neutrinos decouple from the charged leptons and themselves. Weak decoupling commences at temperature scales of a few MeV. The weak interaction mediates an exchange of energy from the electrons and positrons into the neutrino seas

$$\nu + e^{\pm} \leftrightarrow \nu + e^{\pm},\tag{2.1}$$

$$\nu + \overline{\nu} \leftrightarrow e^- + e^+. \tag{2.2}$$

Both of the above processes include charged-current and neutral-current interactions. Electron-flavor neutrinos will experience both charged and neutral-current interactions, while μ and τ -flavor only experience neutral-current. As a result, more heat flows into the electron-flavor sector than either the μ or τ . Three other neutral-current interactions redistribute energy among the neutrino seas

$$\nu_i + \nu_j \leftrightarrow \nu_i + \nu_j, \tag{2.3}$$

$$\nu_i + \overline{\nu}_i \leftrightarrow \nu_i + \overline{\nu}_i,$$
 (2.4)

$$\nu_i + \overline{\nu}_i \leftrightarrow \nu_j + \overline{\nu}_j. \tag{2.5}$$

The above three interactions lead to a "flavor-equilibration" (see figures 7 and 8 in ref. [31]) among the electron and μ/τ flavors.

Weak decoupling concludes at a temperature of a few 10's of keV. The neutrinos will also decouple from the baryons during the Weak Freeze-Out (WFO) epoch. WFO and weak decoupling have a significant overlap in time. However, due to the large number of neutrinos compared to baryons, WFO and weak decoupling are not simultaneous. We monitor the change in the neutron-to-proton ratio of the baryons by calculating six neutron-to-proton rates, schematically given as

$$\nu_e + n \leftrightarrow p + e^-, \tag{2.6}$$

$$e^+ + n \leftrightarrow p + \overline{\nu}_e,$$
 (2.7)

$$n \leftrightarrow p + \overline{\nu}_e + e^-. \tag{2.8}$$

We do not consider the energy and entropy flow from the baryon component into the neutrino seas as this is a small change compared to the entropies of the neutrino seas and plasma.

As the temperature continues to decrease, the electron-positron pairs will annihilate into photons during the eponymous electron-positron annihilation epoch. The last freeze-out epoch is Nuclear Freeze-Out (NFO), when the nuclear abundances go out of nuclear statistical equilibrium and obtain their primordial values. For our purposes, the physics in e^{\pm} -annihilation and NFO are identical in the standard and SI ν scenarios. Although the physics is distinct, the preceding four freeze-out epochs are not temporally distinct. They overlap with one another and require computational tools to model the physics.

2.2 Numerics

At high temperatures, weak interactions keep the neutrinos in thermal and chemical equilibrium with the electromagnetic plasma, i.e., $T_{\nu} = T$. The time derivative of the plasma temperature T is based off of eq. (D28) in [32]

$$\frac{dT}{dt} = -3H \left(\frac{d\rho_{\rm pl}}{dT} \right)^{-1} \left(\rho_{\rm pl} + P_{\rm pl} - \frac{1}{3H} \frac{dQ}{dt} \Big|_{T} \right) \tag{2.9}$$

where $\rho_{\rm pl}$ is the energy density of the plasma (less baryons), $P_{\rm pl}$ is the pressure exerted by all plasma components, $dQ/dt|_T$ is the plasma heat gained/lost from microphysics, and $d\rho_{\rm pl}/dT$ is the temperature derivative of the plasma components (including baryons) [33]. When calculating the electromagnetic energy densities, we implement finite temperature QED effects to the electromagnetic equation of state as explained in [34–36] (see ref. [37] for a detailed analysis of the finite-temperature QED problem in the early universe). At high temperatures, the plasma consists of photons, electrons, positrons, neutrinos, and baryons.

We begin the weak decoupling process at 10 MeV by dissociating the electromagnetic components from the neutrino seas. The electromagnetic plasma temperature continues to evolve according to eq. (2.9) without neutrinos. In the standard scenario, we evolve the neutrino occupation fractions $f_i(\epsilon)$, $i = e, \mu, \tau$ using a weak-interaction collision operator

$$\mathcal{C}_{j}[f_{i}(\epsilon_{1})]\Big|_{\epsilon_{1}=E_{1}/T_{cm}} = \frac{1}{2E_{1}} \int \frac{d^{3}p_{2}}{(2\pi)^{3}2E_{2}} \frac{d^{3}p_{3}}{(2\pi)^{3}2E_{3}} \frac{d^{3}p_{4}}{(2\pi)^{3}2E_{4}} \langle |\mathcal{M}_{j}|^{2} \rangle \delta^{(4)}(P_{1} + P_{2} - P_{3} - P_{4}) \\
\times \left[(1 - f^{(1)})(1 - f^{(2)})f^{(3)}f^{(4)} - f^{(1)}f^{(2)}(1 - f^{(3)})(1 - f^{(4)}) \right], \tag{2.10}$$

where j indicates the collision type corresponding to a reaction in eqs. (2.1)–(2.5). P_k is the four momentum for particle k and $\langle |\mathcal{M}_j|^2 \rangle$ is the amplitude for reaction j (see table I in ref. [31]). We use the shorthand notation $f^{(k)} \equiv f(\epsilon_k)$, k = 1, 2, 3, 4, to denote the fermion occupation numbers for either neutrinos or charged leptons, where the latter is always a FD distribution

$$f_{e^{\pm}}(\epsilon) = \frac{1}{\exp\left(\epsilon \frac{T_{\text{cm}}}{T} \pm \phi_e\right) + 1},\tag{2.11}$$

and ϕ_e is the electron degeneracy parameter defined below. There exists an implicit subscript on $f^{(k)}$ in eq. (2.10) to denote either the flavor (neutrino or antineutrino) or the charged lepton (electron or positron) depending on the collision j. We can calculate the heat flow from the

plasma to the neutrino seas by integrating over the collision terms involving the charged leptons

$$\left. \frac{\partial \rho_{\nu}}{\partial t} \right|_{a} = \frac{T_{\rm cm}^{4}}{2\pi^{2}} \sum_{i=1}^{6} \int d\epsilon \, \epsilon^{3} \{ \mathcal{C}_{\nu e}[f_{i}(\epsilon)] + \mathcal{C}_{e^{-}e^{+}}[f_{i}(\epsilon)] \}. \tag{2.12}$$

Equation (2.12) communicates the change to the plasma using the $dQ/dt|_T$ term in eq. (2.9). Therefore, the final expression for the heat gain/lost due to microphysics is

$$\frac{dQ}{dt}\Big|_{T} = \frac{\partial \rho_{\rm pl}}{\partial t}\Big|_{\rm Nuc} - \frac{\partial \rho_{\nu}}{\partial t}\Big|_{q},\tag{2.13}$$

where the first term is the heat gained from nucleosynthesis, and the minus sign indicates the plasma loses energy to the neutrino seas during weak decoupling.

The only terms in the evolution for the neutrino occupation numbers are the collision operators, i.e.,

$$\frac{df_i(\epsilon)}{dt} = \sum_j C_j[f_i(\epsilon)]. \tag{2.14}$$

We only evolve the occupation numbers of the neutrinos after the universe has reached a temperature of $10 \,\mathrm{MeV}$. When the neutrinos decouple in the standard scenario, they do not follow an equilibrium distribution and so there is no need to evolve temperatures or degeneracy parameters of the neutrino components. $T_{\rm cm}$ acts as an energy scale for the neutrinos so that we may calculate energy density quantities, e.g., eq. (2.12).

Equation (2.9) is derived from conservation of energy [32], but does not conserve particle number. However, we do implement conservation of charge by evolving the electron degeneracy parameter

$$\phi_e \equiv \frac{\mu_{e^-}}{T},\tag{2.15}$$

for electron chemical potential μ_{e^-} . The positron chemical potential is equal in magnitude and opposite in sign if we assume chemical equilibrium between the electrons and positrons. We evolve ϕ_e with time by ensuring electrons and positrons maintain FD distributions and the difference of the two number densities is equal to the number density of protons (both free and those bound in nuclei)

$$n_{e^{-}} - n_{e^{+}} = n_b \sum_{i} Z_i Y_i, \tag{2.16}$$

for baryon number density n_b , atomic numbers Z_i , and nuclear abundances $Y_i \equiv n_i/n_b$. We do not explicitly evolve the degeneracy parameters for the nuclei, but instead evolve their abundances Y_i through the nuclear reaction network with an example equation

$$\frac{dY_i}{dt} = \sum_{i,k,l} \left\{ \frac{Y_k^{N_k} Y_l^{N_l}}{N_k! N_l!} [kl]_{ij} - \frac{Y_i^{N_i} Y_j^{N_j}}{N_i! N_j!} [ij]_{kl} \right\}, \tag{2.17}$$

where $N_{i,j,k,l}$ are the number of each nucleus in the reaction i(j,k)l, $[kl]_{ij}$ is the reaction rate coefficient to create nucleus i, and $[ij]_{kl}$ is the reverse reaction rate coefficient [32]. The

¹We have switched which variable we hold constant in our derivatives with respect to time, either the plasma temperature T or the scale factor a. Although the distinction is important in a thermodynamic sense, T can be parameterized using a implying $d\rho_{\nu}/dt|_{a} = d\rho_{\nu}/dt|_{T}$.

comoving number of protons changes as the weak-charged-current reactions change neutrons into protons, and vice-versa. We use eqs. (19)–(24) in ref. [38] to calculate the rates, which are input into eq. (2.17). Our rate expressions are single integrals over the neutrino energy. We can use either FD expressions or out-of-equilibrium occupation fractions to characterize the neutrino distribution.

The last quantity to evolve is the scale factor with the Friedmann equation

$$H \equiv \frac{1}{a} \frac{da}{dt} = \sqrt{\frac{8\pi}{3m_{\rm pl}^2} \rho_{\rm tot}},\tag{2.18}$$

which defines the Hubble expansion rate H. $m_{\rm pl}$ is the Planck mass, and $\rho_{\rm tot}$ is the total energy density of the universe: photons, electrons, positrons, neutrinos, baryons/nuclei, dark radiation, dark matter, and dark energy. In practice, we ignore the contribution from dark matter and dark energy as they are negligible during the BBN epoch.

2.2.1 Computational code

Public BBN codes exist, see refs. [39–41]. We use our code BURST based off of refs. [31, 42]. We integrate the coupled ordinary differential equations for T, ϕ_e , a, $\{Y_i\}$, $\{f_i(\epsilon_j)\}$ with respect to the coordinate time t. Our calculations commence at $T_{\rm cm}=30\,{\rm MeV}$ and terminate at $T_{\rm cm}=1\,{\rm keV}$. We begin calculating the neutrino collision integrals at $T_{\rm cm}=10\,{\rm MeV}$. We integrate the nuclear reaction network at all times.

2.2.2 Results in the standard scenario

In the standard scenario, we find $N_{\rm eff} = 3.044$, and the following abundances

$$Y_{\rm P} = 0.2478,$$
 (2.19)

$$D/H = 2.624 \times 10^{-5}, \tag{2.20}$$

for a baryon density $\omega_b = 0.02226$, consistent with ref. [43], and a neutron lifetime $\tau_n = 885.1 \,\mathrm{s}$. Our value for primordial lithium is $^7\mathrm{Li/H} = 4.375 \times 10^{-10}$. We caution that the abundances are dependent on the nuclear reaction rates, and so the above quantities should be taken as a baseline when compared to the SI ν scenario, and not absolute predictions.

3 Lepton symmetric initial conditions

3.1 Neutrino transport with self-interactions

With self-interactions, we need to differentiate between two different epochs/phenomena. We will term the process of neutrinos decoupling from the electromagnetic plasma "weak decoupling", in accordance with the terminology used in the standard scenario. When neutrinos decouple from each other, we will call this process "neutrino decoupling". Weak and neutrino decoupling are contemporaneous in the standard model, but occur on vastly different time/energy scales in the SI ν scenario. In our model, we assume that the self-interactions keep the neutrinos in a FD distribution throughout weak decoupling. This neutrino distribution differs from the electron/positron FD distribution in both number and energy density. For lepton-symmetric initial conditions, the FD distribution is identical for neutrinos and anti-neutrinos and we characterize it using a temperature T_{ν} and degeneracy quantity

$$\eta_{\nu} = \frac{\mu_{\nu}}{T_{\nu}} \tag{3.1}$$

for neutrino chemical potential μ_{ν} . As the universe evolves through weak decoupling, there will be a transfer of both energy and particle number to the neutrino seas through the weak interactions. The self interactions only thermalize the neutrino seas by exchanging energy among the constituent particles. These interactions neither create nor destroy neutrino number through communication with the electromagnetic plasma. As a result, energy and number are conserved in the SI ν scenario, unlike how we conserve energy and charge for the electromagnetic plasma components in eqs. (2.9) and (2.16). We must evolve T_{ν} and η_{ν} using the definitions of energy and number density

$$n(T_{\nu}, \eta_{\nu}) = N_{\nu} \frac{T_{\nu}^{3}}{2\pi^{2}} \int d\epsilon \, \epsilon^{2} f^{(\text{eq})}(\epsilon; \eta_{\nu})$$

$$\rho(T_{\nu}, \eta_{\nu}) = N_{\nu} \frac{T_{\nu}^{4}}{2\pi^{2}} \int d\epsilon \, \epsilon^{3} f^{(\text{eq})}(\epsilon; \eta_{\nu})$$

$$\Longrightarrow \begin{cases} T_{\nu} = T_{\nu}(n, \rho) \\ \eta_{\nu} = \eta_{\nu}(n, \rho) \end{cases}, \tag{3.2}$$

where we write T_{ν} and η_{ν} as functions of n and ρ , and the FD expression $f^{(eq)}(\epsilon;\eta_{\nu})$ is

$$f^{(eq)}(\epsilon; \eta_{\nu}) = \frac{1}{e^{\epsilon - \eta_{\nu}} + 1}.$$
(3.3)

In eq. (3.2), N_{ν} is the number of particle species and is equal to 6 (ν_e , $\overline{\nu}_e$, ν_{μ} , $\overline{\nu}_{\mu}$, ν_{τ} , $\overline{\nu}_{\tau}$) in the non-degenerate SI ν scenario. If we add energy or number to the neutrino seas, we change both T_{ν} and η_{ν} via the definitions of energy and number density

$$\frac{d\chi}{dt} = \frac{\partial \chi}{\partial T_{\nu}} \frac{dT_{\nu}}{dt} + \frac{\partial \chi}{\partial \eta_{\nu}} \frac{d\eta_{\nu}}{dt},\tag{3.4}$$

where χ denotes either ρ or n. Therefore, we find the time derivative of T_{ν} to be

$$\frac{dT_{\nu}}{dt} = -HT_{\nu} + T_{\nu} \frac{n_{,\eta} \frac{\partial \rho}{\partial t} \Big|_{a} - 3T_{\nu} n \frac{\partial n}{\partial t} \Big|_{a}}{4\rho n_{,\eta} - 9T_{\nu} n^{2}},$$
(3.5)

and the time derivative of η_{ν}

$$\frac{d\eta_{\nu}}{dt} = \frac{4\rho \frac{\partial n}{\partial t} \bigg|_{a} - 3n \frac{\partial \rho}{\partial t} \bigg|_{a}}{4\rho n_{,n} - 9T_{\nu} n^{2}},\tag{3.6}$$

where $\partial n/\partial t|_a$ is the number density added from out-of-equilibrium weak decoupling, $\partial \rho/\partial t|_a$ is the energy density added, and $n_{,\eta}$ is the following expression

$$n_{,\eta} = N_{\nu} \frac{T_{\nu}^{3}}{\pi^{2}} \int d\epsilon \, \epsilon f^{(\text{eq})}(\epsilon; \eta_{\nu}). \tag{3.7}$$

We have written T_{ν} and η_{ν} as functions of energy and number density in eq. (3.2). Although ρ and n have familiar meanings in an out-of-equilibrium system, temperature and chemical potential (i.e., degeneracy parameter) do not have the same thermodynamic meaning as they would in an equilibrium system. Simply stated, T_{ν} and η_{ν} are parameters for energy and number distributions. Equations (3.5) and (3.6) give the equations of motion for the two parameters and are consistent with the definitions of n and ρ in eq. (3.2). The electromagnetic plasma acts as a heat source for the neutrinos, but the lack of a tight-coupling between the two systems precludes the equivalence of T_{ν} and η_{ν} with the thermodynamic

variables of temperature and degeneracy parameter of the grand canonical ensemble. Nevertheless, we will colloquially refer to T_{ν} and η_{ν} as temperature and degeneracy parameter, respectively, throughout this manuscript.

There are two weak interaction collision terms we use in the $\mathrm{SI}\nu$ scenario

$$\nu + e^{\pm} \leftrightarrow \nu + e^{\pm},\tag{3.8}$$

$$\nu + \overline{\nu} \leftrightarrow e^- + e^+, \tag{3.9}$$

with collision terms $C_{\nu e}$ and $C_{e^-e^+}$, respectively. $C_{\nu e}$ and $C_{e^-e^+}$ are the same collision operators for the standard scenario of out-of-equilibrium neutrino spectra (see appendix C in ref. [31]). For our purposes, we do not evolve the individual occupation fractions, $f_{\nu_i}(\epsilon)$, of the neutrino spectra. Instead, we use the FD expression $f^{(eq)}(\epsilon; \eta_{\nu})$ for both terms and integrate over ϵ to find the total added neutrino number and energy density for a given time step. Note that $C_{\nu e}$ preserves the neutrino number and changes the energy, while $C_{e^-e^+}$ changes both number and energy. Therefore, the number and energy density added during the out-of-equilibrium weak decoupling is

$$\left. \frac{\partial n}{\partial t} \right|_{a} = \frac{T_{\nu}^{3}}{2\pi^{2}} \sum_{i=1}^{6} \int d\epsilon \, \epsilon^{2} \mathcal{C}_{e^{-}e^{+}}[f^{(\text{eq})}(\epsilon; \eta_{\nu})], \tag{3.10}$$

$$\left. \frac{\partial \rho}{\partial t} \right|_{a} = \frac{T_{\nu}^{4}}{2\pi^{2}} \sum_{i=1}^{6} \int d\epsilon \, \epsilon^{3} \{ \mathcal{C}_{\nu e}[f^{(\text{eq})}(\epsilon; \eta_{\nu})] + \mathcal{C}_{e^{-}e^{+}}[f^{(\text{eq})}(\epsilon; \eta_{\nu})] \}. \tag{3.11}$$

Equation (3.11) is a copy of eq. (2.12) except we use T_{ν} instead of $T_{\rm cm}$ for the energy scale. There is neither number nor energy density added to the neutrino seas after weak decoupling concludes. At this point, eqs. (3.5) and (3.6) reduce to

$$\frac{dT_{\nu}}{dt} = -HT_{\nu},\tag{3.12}$$

$$\frac{d\eta_{\nu}}{dt} = 0, (3.13)$$

which are the free-streaming conditions for relativistic particles.

3.2 Results

3.2.1 Neutrino spectra

Figure 1 gives the relative change of the neutrino occupation fractions from non-degenerate FD equilibrium, i.e.,

$$\delta f(\epsilon) \equiv \frac{f(\epsilon) - f^{(eq)}(\epsilon; 0)}{f^{(eq)}(\epsilon; 0)}, \tag{3.14}$$

versus the dimensionless comoving energy. The dashed lines are the out-of-equilibrium neutrino spectra for e-flavor neutrinos (green) and either μ or τ -flavor (red) which are degenerate in our Boltzmann scenario. The solid blue line is the degenerate FD equilibrium spectrum for any species of neutrino in the SI ν scenario. The dotted black line at zero represents a non-degenerate spectrum at temperature $T_{\rm cm}$. In either scenario, there exists an overabundance of particles at high ϵ . The positive slope of the SI ν curve corresponds to a higher temperature T_{ν} compared to $T_{\rm cm}$. We compare the energy scales T_{ν} and $T_{\rm cm}$ using the following definition

$$\frac{T_{\nu}}{T_{\rm cm}} - 1 = aT_{\nu} - 1 \equiv \Delta(aT_{\nu}),$$
 (3.15)

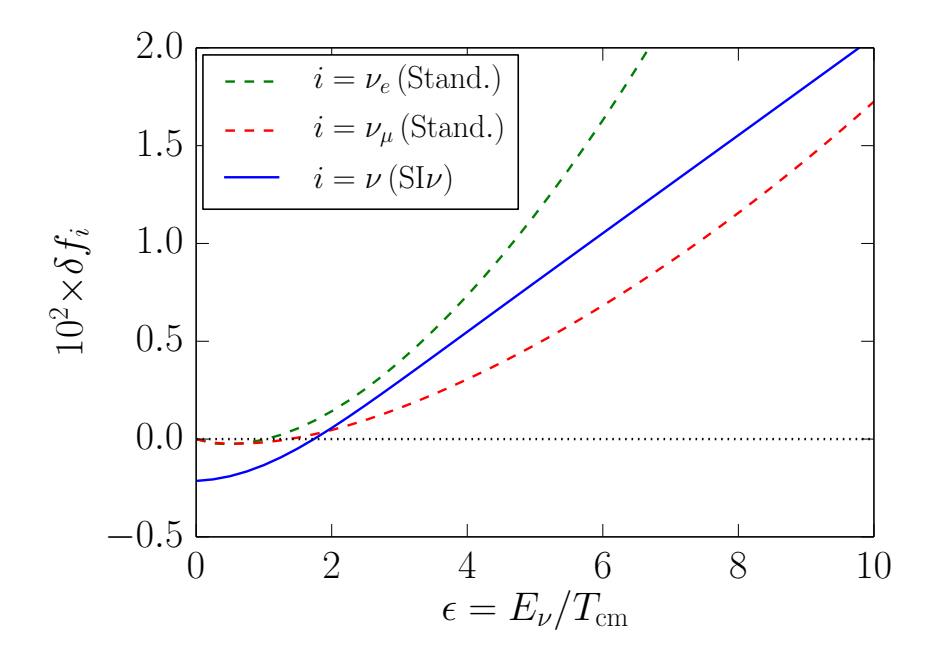


Figure 1. Freeze-out neutrino spectra in the standard scenario (dashed) and the SI ν scenario (solid) plotted against ϵ . In the standard scenario of Boltzmann transport, the green dashed curve is the e flavor and the red dashed curve is either μ or τ . Vertical axis is the relative change to a non-degenerate FD spectrum in eq. (3.14).

where we ascribe a unit conversion between scale factor and temperature such that the product is dimensionless and equal to unity when $T_{\nu} = 10 \,\mathrm{MeV}$. At freeze-out (f.o.), we find

$$\Delta(aT_{\nu})|_{\text{f.o.}} = 2.463 \times 10^{-3},$$
 (3.16)

showing a slight increase in T_{ν} over $T_{\rm cm}$. Conversely, at low ϵ there exists a deficit of particles, which corresponds to a negative degeneracy parameter

$$\eta_{\nu}|_{\text{f.o.}} = -4.282 \times 10^{-3}.$$
 (3.17)

In the standard out-of-equilibrium scenario, the deficit arises from the up-scattering of low-energy neutrinos on higher-temperature charged leptons, given schematically in eq. (3.8). The situation is similar for $SI\nu$, as both elastic scattering and electron-positron annihilation [eq. (3.9)] add energy and a modest number of particles to the neutrino seas. We can explain the behavior in figure 1 by examining eqs. (3.5) and (3.6). The denominator in both equations is positive if $\eta_{\nu} = 0$. If we solve the numerators for the energy added per particle we find

$$\frac{\partial \rho}{\partial n} > \frac{3T_{\nu}n}{n_{,n}} \implies \frac{dT_{\nu}}{dt} > 0,$$
 (3.18)

$$\frac{\partial \rho}{\partial n} < \frac{4\rho}{3n} \implies \frac{d\eta_{\nu}}{dt} > 0,$$
 (3.19)

where we ignore the redshift term for dT_{ν}/dt in eq. (3.5). Assuming non-degenerate statistics,

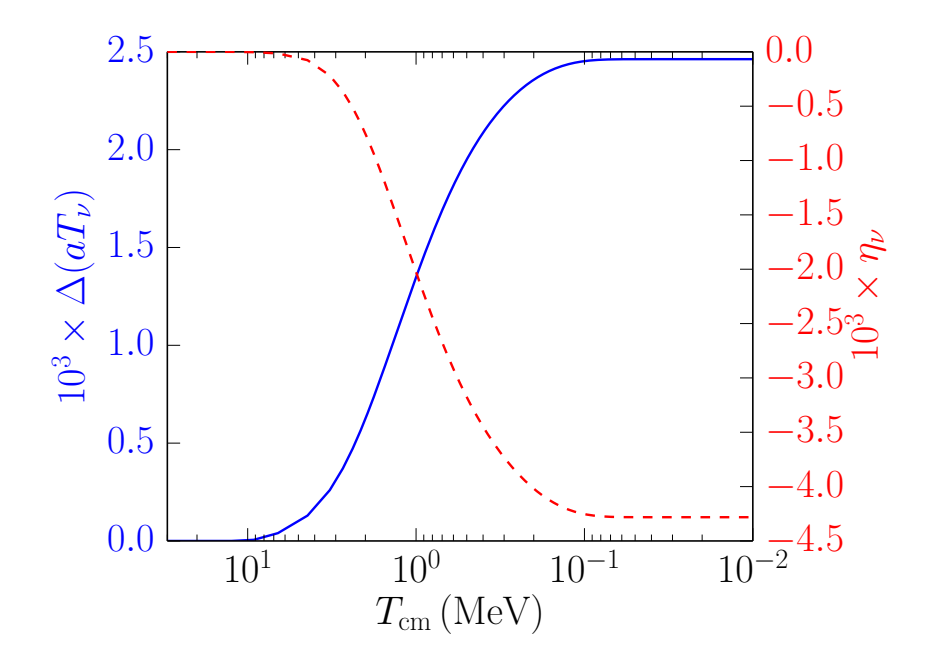


Figure 2. Evolution of $\Delta(aT_{\nu})$ from eq. (3.15) (solid blue curve) and η_{ν} (dashed red curve) plotted against $T_{\rm cm}$.

we calculate

$$\frac{3T_{\nu}n}{n_{,\eta}} \simeq 3.288T_{\nu},$$
 (3.20)

$$\frac{4\rho}{3n} \simeq 4.202T_{\nu}.$$
 (3.21)

Figure 4 in ref. [31] shows that the weak-decoupling induced distortion in the neutrino seas is located at $\epsilon \simeq 5$ in the standard scenario. As this is larger than the two values above, the same energy per particle injection in the SI ν case would imply an increase in T_{ν} over $T_{\rm cm}$ and a decrease in η_{ν} , which is borne out by figure 1.

We have given the values at freeze-out for η_{ν} and $T_{\rm cm}/T_{\nu}$. Figure 2 shows the evolution of $\Delta(aT_{\nu})$ (solid blue line) and η_{ν} (dashed red line) from the initial values of zero to the freeze-out values as a function of $T_{\rm cm}$. The product aT_{ν} and the quantity η_{ν} can only change during weak decoupling, i.e., when the derivatives $\partial n/\partial t|_a$ and $\partial \rho/\partial t|_a$ are non-zero. Figure 2 illustrates the weak-decoupling epoch, starting at a few MeV, and finishing slightly after 100 keV.

Neutrino self-interactions only indirectly influence the heat flow from the plasma into the neutrino seas. Figure 1 shows that the occupation numbers at freeze-out differ between the two scenarios. This is also the case during the entirety of weak decoupling. Modifying the occupation numbers and associated Pauli blocking factors will change the neutrino-charged-lepton scattering rates through the $f^{(k)}$ factors given in eq. (2.10). The SI ν spectrum lies in between the two spectra for e-flavor and μ -flavor in figure 1, implying a slight enhancement (suppression) for scattering between charged leptons and $e(\mu)$ -flavor neutrinos. There is also an enhancement at low ϵ for any flavor for a substantially negative η_{ν} . When calculating the radiation energy density at low temperatures, we find $N_{\rm eff}=3.045$, a small overall increase of 10^{-3} compared to the result in section 2.2. Although we evolve a non-zero degeneracy

parameter, our result for N_{eff} agrees with the $T_{\nu_e} = T_{\nu_{\mu,\tau}}$ model in the last row of table 1 of ref. [44].

3.2.2 Primordial abundances

The calculation for the primordial abundances is nearly identical in the standard and SI ν scenarios. The only difference between the two scenarios is in the neutron-to-proton rates. The SI ν scenario uses FD distributions with T_{ν} and η_{ν} compared to out-of-equilibrium occupation numbers $\{f_{\nu_e,\overline{\nu}_e}(\epsilon)\}$ for the standard scenario. The difference results in small relative changes for $Y_{\rm P}$ and D/H

$$\delta Y_{\rm P} \simeq 4 \times 10^{-4},\tag{3.22}$$

$$\delta(D/H) \simeq 2 \times 10^{-4}.$$
 (3.23)

Both changes are well within observational uncertainties [45, 46]. There exists a slight increase in the ratio $^7\text{Li/H}$ with a relative change of 2×10^{-4} . The increase in all abundances is due to an increase in the neutron-to-proton ratio which results from a decrease in the rate $n(\nu_e, e^-)p$ as there exists fewer ν_e in the SI ν case [47].

4 Dark radiation addition

4.1 Dark radiation parameter

This section and the succeeding one explore cosmological extensions to the SI ν scenario. We begin by considering an addition of dark radiation [48] to the universal energy density. The dark radiation only interacts with the other components through gravitation. Within the computation, only the Hubble expansion rate in eq. (2.18) changes. We parameterize the dark radiation energy density by using the quantity $\delta_{\rm dr}$, introduced in [42]

$$\rho_{\rm dr} = \frac{7\pi^2}{120} T_{\rm cm}^4 \delta_{\rm dr}.\tag{4.1}$$

After electron-positron annihilation terminates, we can calculate the change to $N_{\rm eff}$ by adding $\rho_{\rm dr}$ to $\rho_{\rm rad}$ in eq. (1.5)

$$\Delta N_{\text{eff}}^{(dr)} = \left(\frac{11}{4}\right)^{4/3} \left(\frac{T_{\text{cm}}}{T}\right)_{\text{f.o.}}^{4/3} \delta_{\text{dr}}.$$
 (4.2)

Weak decoupling and QED corrections to the plasma equation of state modify the transfer of entropy from the charged leptons to the photons. The result is a freeze-out ratio $T_{\rm cm}/T$ larger than $(4/11)^{1/3}$, causing $\Delta N_{\rm eff}^{\rm (dr)}$ to be larger than $\delta_{\rm dr}$. The increase is less than 1%, so $\Delta N_{\rm eff}^{\rm (dr)} \approx \delta_{\rm dr}$ to good approximation.

We do a parameter-space scan over δ_{dr} to calculate the changes to the neutrino spectra and primordial abundances in the SI ν scenario.

4.2 Results

4.2.1 Neutrino spectra

By construction, the dark radiation component has no direct effect on neutrino scattering and weak decoupling. When adding extra radiation energy density to the universe, we expect an earlier epoch of weak decoupling precipitated by the more rapid expansion rate. This

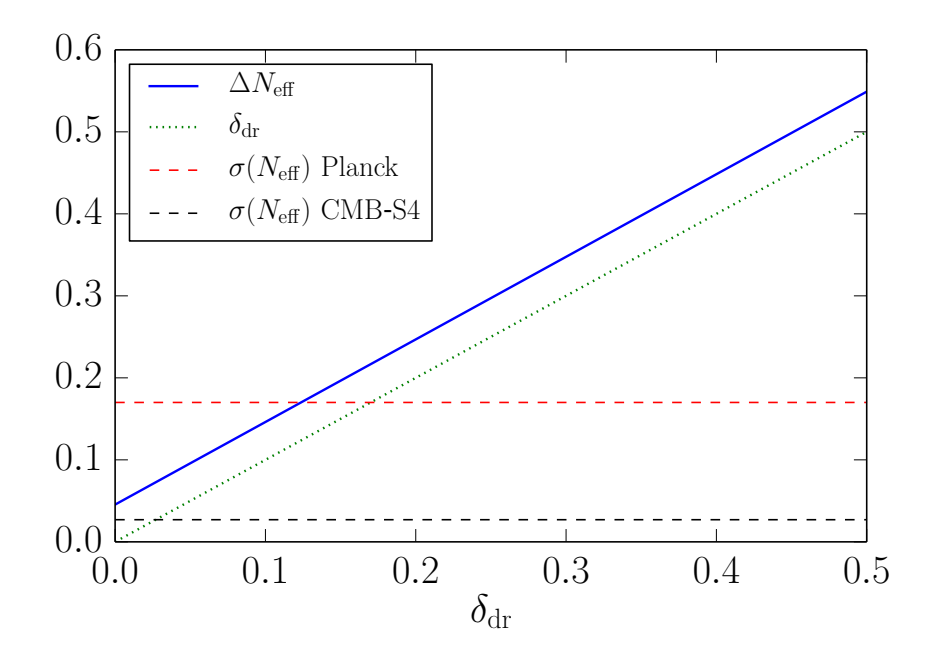


Figure 3. Change in $N_{\rm eff}$ plotted against $\delta_{\rm dr}$.

conclusion is identical for either the standard or $SI\nu$ scenarios. The final freeze-out spectra look similar to the blue curve in figure 1, and the evolution of T_{ν} and η_{ν} are qualitatively the same for the scenarios with and without dark radiation.

In figure 3 we plot four quantities related to $N_{\rm eff}$ against the parameter $\delta_{\rm dr}$. The solid blue curve gives $\Delta N_{\rm eff} \equiv N_{\rm eff} - 3$ and includes neutrino transport, QED corrections, and dark radiation in the SI ν scenario. The dashed green curve is $\delta_{\rm dr}$ and close to the change in $N_{\rm eff}$ from the addition of the dark radiation. The horizontal lines give the 1σ uncertainty in $N_{\rm eff}$ from Planck (dashed red line) [43] and a projection from Cosmic Microwave Background (CMB) Stage IV (dashed black line) [49].

The blue and green lines appear to run parallel to one another in figure 3, suggesting that changes to $N_{\rm eff}$ from neutrino transport/QED corrections and dark radiation add linearly. This conclusion is indeed the case to good precision and is also true in the standard scenario. In models with dark radiation, the non-linear contribution to $\Delta N_{\rm eff}$ comes from a change in the expansion rate which leads to an earlier epoch of weak decoupling and subsequently lowers the amount of heat flow from the plasma into the neutrino seas. This effect changes both the energy density in the neutrino seas and also the ratio $T_{\rm cm}/T|_{\rm f.o.}$ in eq. (4.2). We have verified this behavior by comparing $N_{\rm eff}(\delta_{\rm dr}=0.5)$ to $N_{\rm eff}(\delta_{\rm dr}=1.0)$ in the following manner

$$2 - \frac{N_{\text{eff}}(\delta_{\text{dr}} = 1.0) - N_{\text{eff}}(\delta_{\text{dr}} = 0)}{N_{\text{eff}}(\delta_{\text{dr}} = 0.5) - N_{\text{eff}}(\delta_{\text{dr}} = 0)} \simeq 9 \times 10^{-5},$$
(4.3)

indicating that the degree of non-linearity is small and the blue and green curves in figure 3 are parallel to high precision. The non-linearity grows with increasing $\delta_{\rm dr}$ but is not a factor for modest values of $N_{\rm eff}$. We emphasize this analysis is for the SI ν scenario but is directly applicable to the standard scenario.

4.2.2 Primordial abundances

Increasing δ_{dr} precipitates an earlier epoch of weak freeze-out between the neutrinos and baryons, and results in a higher neutron-to-proton ratio during nuclear freeze-out. Both Y_P

and D/H increase in the presence of an over-abundance of neutrons. We direct the reader to refs. [50, 51] for more information on extra radiation energy density in BBN, and in particular ref. [52] for quantitative scaling forms of the abundances with $\Delta N_{\rm eff}$. Transport and self-interactions do little to modify the scaling forms and instead renormalize the values when $\delta_{\rm dr}=0$. We give specific values of $Y_{\rm P}$ and D/H with relative changes from the standard baseline for the case $\delta_{\rm dr}=0.4009$

$$Y_{\rm P} = 0.2532 \implies \delta Y_{\rm P} = 2.161\% \quad (\delta_{\rm dr} = 0.4009),$$

 $D/H = 2.769 \times 10^{-5} \implies \delta(D/H) = 5.385\% \quad (\delta_{\rm dr} = 0.4009).$ (4.4)

We highlight that eq. (4.4) shows that deuterium, not helium, has a larger relative change with the addition of dark radiation. In fact, this is a general trend in BBN and not specific to the value of $\delta_{\rm dr}$ taken in eq. (4.4). Figure 10 of ref. [52] shows the hyper-sensitivity of D/H to extra energy density. The reason for the result in eq. (4.4) is the dark radiation precipitates an earlier freeze-out of nuclear reaction rates. Given the precision in measuring D/H, any BBN scenario which includes a dark radiation component must consider the impact on deuterium production.

5 Lepton asymmetric initial conditions

We give a second example of a one-parameter extension to the $SI\nu$ scenario by introducing an asymmetry between numbers of neutrinos and anti-neutrinos with the following quantity [53]

$$L_{\nu_i}^{\star} \equiv \frac{n_{\nu_i} - n_{\overline{\nu}_i}}{\frac{2\zeta(3)}{\pi^2} T_{\rm cm}^3}, \quad i = e, \mu, \tau,$$
 (5.1)

where $\zeta(3) = 1.202$ is the Riemann Zeta function of argument 3. The above definition is identical with the standard definition of lepton number

$$L_{\nu_i} = \frac{n_{\nu_i} - n_{\overline{\nu}_i}}{n_{\gamma}},\tag{5.2}$$

at high temperature where $T_{\rm cm}=T$. We use $L_{\nu_i}^{\star}$ as it is a comoving invariant throughout electron-positron annihilation and label it the comoving lepton number to distinguish it from eq. (5.2). If self-interactions violate flavor conservation, than we would expect the comoving lepton number to be the same in all three flavors. Additionally, if self-interactions violate lepton number, we would expect $L_{\nu_i}^{\star}=0$ for all flavors at the commencement of BBN. We will consider the SI ν scenario of flavor-violation and lepton-number conservation in this section. Therefore, we only use a single quantity L_{ν}^{\star} to describe the asymmetry for any flavor.

5.1 Differences in implementation with symmetric scenario

Neutrinos and anti-neutrinos will evolve uniquely in the SI ν scenario with asymmetric initial conditions. In general, we need temperature and degeneracy quantities for the anti-neutrinos, namely, $T_{\overline{\nu}}$ and $\eta_{\overline{\nu}}$. The Lagrangian in eq. (1.1) allows for t-channel scattering between neutrinos and anti-neutrinos, so the interaction

$$\nu + \overline{\nu} \leftrightarrow \nu + \overline{\nu},$$
 (5.3)

holds the two seas in thermal equilibrium, implying $T_{\nu} = T_{\overline{\nu}}$. Equation (5.3), however, does not hold the two seas in chemical equilibrium. As a result, our model of SI ν with

lepton degeneracy only requires the introduction of one new variable, namely $\eta_{\overline{\nu}}$. The set of variables $\{T_{\nu}, \eta_{\nu}, \eta_{\overline{\nu}}\}$ evolve in accordance with the definitions of energy and number density for neutrinos and anti-neutrinos. The expressions for $n_{\nu}(T_{\nu}, \eta_{\nu})$ and $n_{\overline{\nu}}(T_{\nu}, \eta_{\overline{\nu}})$ are identical to eq. (3.2), except now $N_{\nu} = 3$ for three flavors of neutrinos/anti-neutrinos. ρ_{ν} and $\rho_{\overline{\nu}}$ follow from analogy.

The asymmetry in the system implies there will be heat flow between the neutrinos and anti-neutrinos. Although the weak interaction can precipitate such a heat flow, the t-channel $SI\nu$ interaction will be much more efficient and will thermally equilibrate the two seas instantaneously. To account for this fact, we need to supplement the weak collision terms with an equilibration term $d\mathcal{E}/dt$

$$\frac{\partial \rho_{\nu}}{\partial t} \bigg|_{a} = \frac{T_{\nu}^{4}}{2\pi^{2}} \sum_{i=1}^{3} \int d\epsilon \, \epsilon^{3} \{ \mathcal{C}_{\nu e}[f^{(\text{eq})}(\epsilon; \eta_{\nu})] + \mathcal{C}_{e^{-}e^{+}}[f^{(\text{eq})}(\epsilon; \eta_{\nu})] \} + \frac{d\mathcal{E}}{dt}, \tag{5.4}$$

$$\frac{\partial \rho_{\overline{\nu}}}{\partial t}\Big|_{a} = \frac{T_{\nu}^{4}}{2\pi^{2}} \sum_{i=1}^{3} \int d\epsilon \, \epsilon^{3} \{ \mathcal{C}_{\nu e}[f^{(\text{eq})}(\epsilon; \eta_{\overline{\nu}})] + \mathcal{C}_{e^{-}e^{+}}[f^{(\text{eq})}(\epsilon; \eta_{\overline{\nu}})] \} - \frac{d\mathcal{E}}{dt}. \tag{5.5}$$

The equilibration term is a weighted average of the energy and number flows due to the weak interaction. If we group the weak-collision terms into $d\rho_{\nu}/dt|_{\rm w}$ and $d\rho_{\overline{\nu}}/dt|_{\rm w}$, we find

$$\frac{d\mathcal{E}}{dt} = \left[4n_{\nu,\eta}n_{\overline{\nu},\eta}(\rho_{\nu} + \rho_{\overline{\nu}}) - 9T_{\nu}(n_{\nu}^{2}n_{\overline{\nu},\eta} + n_{\overline{\nu}}^{2}n_{\nu,\eta})\right]^{-1} \\
\times \left\{3T_{\nu}\left[4(n_{\nu}\rho_{\overline{\nu}}n_{\overline{\nu},\eta} - n_{\overline{\nu}}\rho_{\nu}n_{\nu,\eta}) + 9T_{\nu}n_{\nu}n_{\overline{\nu}}(n_{\nu} - n_{\overline{\nu}})\right]\frac{\partial n_{\nu}}{\partial t}\Big|_{a} \\
+4n_{\nu,\eta}n_{\overline{\nu},\eta}\left(\rho_{\nu}\frac{\partial\rho_{\overline{\nu}}}{\partial t}\Big|_{w} - \rho_{\nu}\frac{\partial\rho_{\overline{\nu}}}{\partial t}\Big|_{w}\right) + 9T_{\nu}\left(n_{\overline{\nu}}^{2}n_{\nu,\eta}\frac{\partial\rho_{\nu}}{\partial t}\Big|_{w} - n_{\nu}^{2}n_{\overline{\nu},\eta}\frac{\partial\rho_{\overline{\nu}}}{\partial t}\Big|_{w}\right)\right\}. (5.6)$$

In writing eq. (5.6), we have set $\partial n_{\overline{\nu}}/\partial t|_a = \partial n_{\nu}/\partial t|_a$ as the weak-collision terms conserve lepton number. Those number-flow terms are analogous to eq. (3.10). The derivatives for T_{ν} , η_{ν} , and $\eta_{\overline{\nu}}$ follow from eqs. (3.5) and (3.6).

Initially at high temperature, neutrinos and anti-neutrinos are in thermal equilibrium with the plasma and $T_{\nu} = T$. In addition, the weak interaction ensures neutrinos and anti-neutrinos are in chemical equilibrium and have degeneracy parameters equal in magnitude and opposite in sign. The equation

$$L_{\nu}^{\star} = \frac{1}{12\zeta(3)} (\pi^2 \xi + \xi^3) \tag{5.7}$$

relates the comoving lepton number to the degeneracy parameter [23]. We begin the calculation by setting $\eta_{\nu} = \xi$ and $\eta_{\overline{\nu}} = -\xi$.

5.2 Results

5.2.1 Neutrino spectra

We give an example of an asymmetric SI ν calculation with $L_{\nu}^{\star} = 2.897 \times 10^{-3}$ in figure 4. The two curves of figure 4 show the evolution of the degeneracy parameters for neutrinos (solid blue curve) and anti-neutrinos (solid red curve) as a function of $T_{\rm cm}$. These two curves evolve similarly albeit with a noticeable offset due to the initial asymmetry. Figure 4 clearly shows

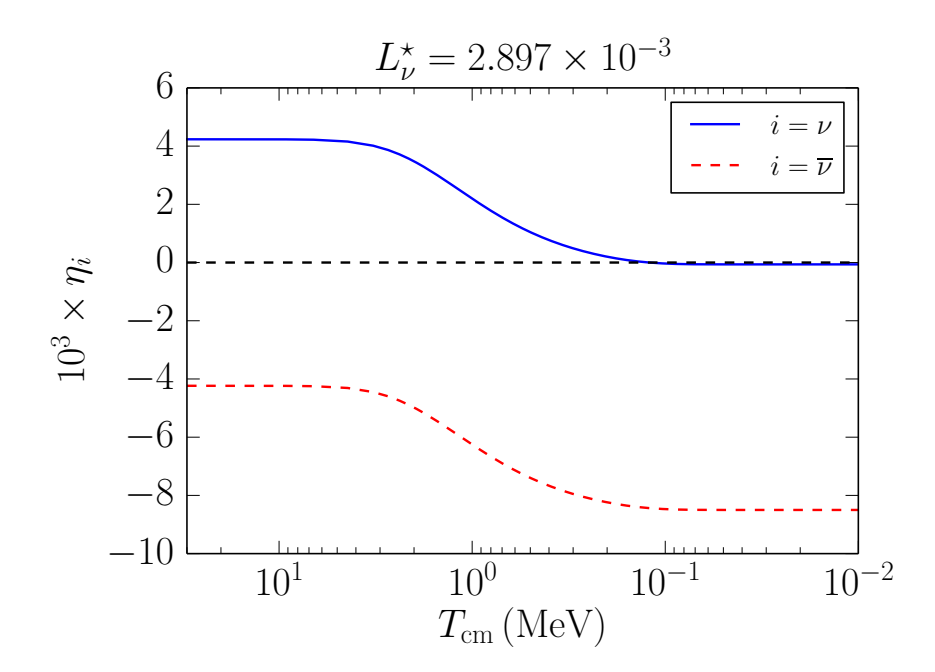


Figure 4. Evolution of η_i , $i = \nu, \overline{\nu}$ as a function of $T_{\rm cm}$. The comoving lepton number is $L_{\nu}^{\star} = 2.897 \times 10^{-3}$.

the composite neutrino/anti-neutrino system is not in equilibrium as $\eta_{\nu} \neq -\eta_{\overline{\nu}}$ once weak decoupling begins. We do not show the evolution of T_{ν} as its behavior is similar to that of T_{ν} in the lepton-symmetric case in figure 2. The paucity of anti-neutrinos leads to a suppression of the Pauli blocking factors in the weak collision terms, and therefore an increase in the scattering rates of charged leptons with anti-neutrinos. Conversely, the overabundance of neutrinos enhances the Pauli blocking factors and decreases those scattering rates. The two effects together imply $d\mathcal{E}/dt > 0$. Overall, the increase in the anti-neutrino scattering rates and the decrease in the neutrino rates nearly cancel and the end result is the evolution of T_{ν} in the lepton-asymmetric case does induce a larger heat flow than the lepton-symmetric case, but the difference is below the resolution of the plot for T_{ν} in figure 2.

We have shown results for the neutrino parameters in the case $L_{\nu}^{\star} > 0$. If $L_{\nu}^{\star} < 0$, then we are in the opposite CP system and the results corresponding to figure 4 would be CP conjugates. The quantity N_{eff} does change in an asymmetric scenario as this system has a larger energy density. However, N_{eff} only has sensitivity to the magnitude of L_{ν}^{\star} . Both the larger energy density from degenerate FD statistics and neutrino energy transport are symmetrical for $\pm L_{\nu}^{\star}$. Therefore, N_{eff} is immune to the sign of L_{ν}^{\star} .

5.2.2 Primordial abundances

As opposed to $N_{\rm eff}$, the primordial abundances are indeed sensitive to the sign of L_{ν}^{\star} . The neutrino spectra are inputs into the neutron-to-proton rates and therefore change the evolution of the neutron-to-proton ratio. We execute a parameter space scan over L_{ν}^{\star} to examine how the lepton asymmetry affects the primordial abundances in the SI ν scenario. Figure 5 shows $Y_{\rm P}$ as a function of $|L_{\nu}^{\star}|$, where the blue curve gives $Y_{\rm P}$ for $L_{\nu}^{\star} > 0$ and the red curve gives $Y_{\rm P}$ for $L_{\nu}^{\star} < 0$. We only show $Y_{\rm P}$ in figure 5, but the other abundances have similar shapes as seen in figure 14 in ref. [53]. In particular, D/H follows qualitatively the same

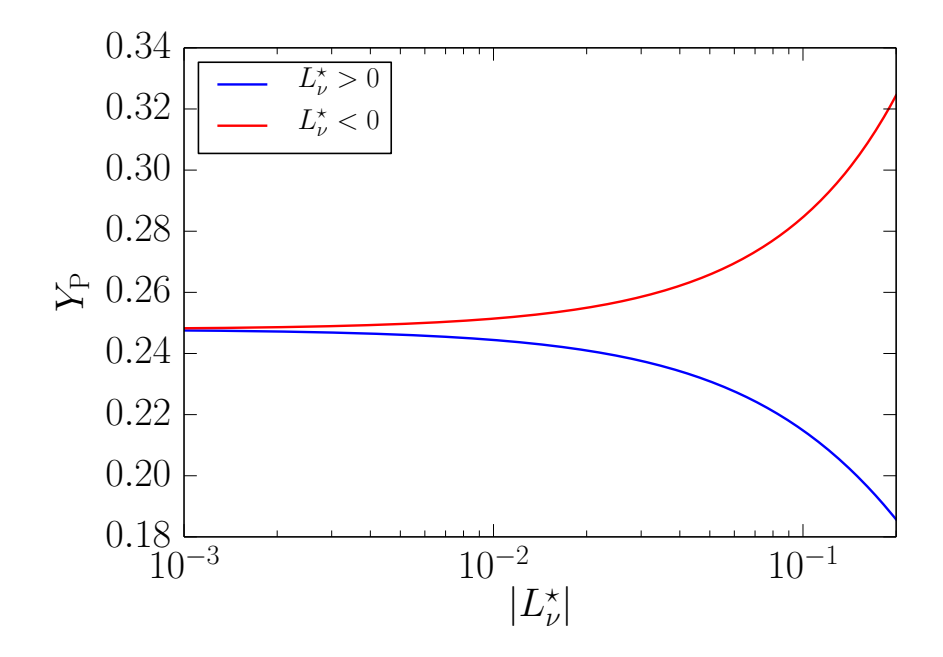


Figure 5. $Y_{\rm P}$ plotted against $|L_{\nu}^{\star}|$ [eq. (5.1)] in the SI ν scenario.

shape as the curves in figure 5 and has a relative change of $\sim 1/2$ as compared to $Y_{\rm P}$ at all values of L_{ν}^{\star} .

Before we conclude, we provide an example model with specific values. If we desire to decrease the helium mass fraction by 10%, we would need a positive comoving lepton number of $L_{\nu}^{\star} \simeq 0.073$. A 10% change in $Y_{\rm P}$ would be difficult to reconcile with current observational bounds [45]. The extra energy density from this value of comoving lepton number translates to $\Delta N_{\rm eff} = 0.06$, which is consistent with ref. [43]. We conclude that $Y_{\rm P}$ has the potential to be a better probe for L_{ν}^{\star} than $N_{\rm eff}$. Our conclusion is for the SI ν scenario and is directly applicable to the standard scenario extension with lepton asymmetry.

6 Conclusions

6.1 Summary

Self-interacting neutrinos constitute a model of Beyond Standard Model (BSM) physics with implications for BBN. Neutrinos go out of thermal and chemical equilibrium during BBN in the standard scenario. Figure 1 shows that these deviations from equilibrium are small, although potentially detectable in future measurements of $N_{\rm eff}$ [49]. Self-interacting neutrinos have little influence on the magnitude of the deviations, and instead reshuffle the neutrino energy among the flavors while preserving the general shape of the spectra. Figure 2 shows that self-interactions modify the spectral parameters by a few parts in 10^3 . Although the physics governing neutrino interactions is different, the standard and $SI\nu$ scenarios do not predict any substantial differences for cosmological observables/parameters at present or future precision [see eqs. (3.22) and (3.23)].

We have extended our BSM model to include self-interactions and dark radiation. With the inclusion of extra radiation energy density, weak decoupling terminates at an earlier epoch and less heat flows from the electromagnetic plasma to the neutrino seas. Equation (4.3) shows the change in neutrino energy density caused by the earlier freeze-out is small. As

a result, self-interactions perturb the neutrino seas in much the same manner as they did without the addition of the dark radiation. Figure 3 shows how $N_{\rm eff}$ changes with the addition of dark radiation, which is nearly an incoherent sum of the extra energy density and the effects from weak decoupling. Although figure 3 is for the SI ν scenario, $N_{\rm eff}$ behaves in quantitatively the same manner for the one-parameter extension to the standard scenario.

Finally, we extended the SI ν scenario to include lepton asymmetry. In the class of models we explore, the self-interactions always maintain flavor-identical distributions among the neutrino and anti-neutrino seas. The flavor-independence of the self-interactions results in the lepton numbers necessarily being identical to one another for the three flavors. The difference between this scenario and the ones with symmetric initial conditions is that the neutrino and anti-neutrino components can have different spectra. Figure 4 shows different evolutions for the degeneracy parameters in a SI ν scenario where $L^{\star}_{\nu}=2.897\times10^{-3}$. Although the degeneracy parameters undergo different evolutions compared to the symmetric scenario, the net change from the initial starting point is still a few parts in 10^3 . As a result, predictions on cosmological parameters/observables mainly scale with the presence of a non-zero L^{\star}_{ν} , and self-interactions produce higher-order effects. Figure 5 gives the primordial mass fraction of 4 He as a function of L^{\star}_{ν} in the SI ν scenario. Lepton degeneracy sources an increasing (decreasing) $Y_{\rm P}$ with decreasing (increasing) L^{\star}_{ν} while self-interactions simply translate the curves to slightly higher values.

6.2 Discussion

The motivation for this work was to determine the dynamics of weak decoupling and primordial nucleosynthesis in the presence of $SI\nu$. Our impetus for this decision is two-fold. First, the neutrinos experience kinetic evolution during this epoch, as scattering rates are neither large enough to maintain equilibrium nor small enough to preclude thermal contact. If new neutrino physics manifests during BBN, standard-model physics will not be able to erase these signals. Second, cosmological parameters/observables directly influenced by the physics of the BBN epoch have already been measured. Advances in precision on $\{N_{\rm eff}, Y_{\rm P}, {\rm D/H}\}$ will either place stronger constraints or reveal signatures of new physics. Coupled together, the kinetic regime and the ability to make measurements which provide diagnostics of the physics operating during this epoch provide researchers with a tool to explore new physical theories.

Our intent for this work was to quantify how self-interactions, and solely self-interactions, modify the neutrino spectra and concomitant light-element synthesis. Section 3 presents the results for the SI ν scenario which amount to less than a 1% change from the standard BBN scenario. The same level of relative changes between the standard and SI ν scenarios occur when we add dark radiation or lepton asymmetry to BBN. We conclude that BBN does not provide any additional constraints on a scenario with only self-interacting neutrinos.

We chose a limited class of $SI\nu$ models for this work. Namely, we operate in the following $SI\nu$ framework: (1) the interaction matrix, g_{ij} in eq. (1.2), is agnostic to any particular flavor; (2) the self-interactions are CP-symmetric; (3) φ is a complex scalar; (4) the mass of φ is large compared to BBN energy scales; and finally (5), the neutrinos stay self-coupled throughout BBN. We contemplate the repercussions if we relax each one of these limitations in turn.

Our choice for g_{ij} forced all flavors of neutrinos to have the same distribution. Had we set the off-diagonal terms of g_{ij} to zero, then we would have needed separate parameters T_{ν_i} and η_{ν_i} for each flavor. Given how little self-interactions changes cosmological parameters/observables, we do not expect this class of models to alter our conclusions significantly.

Table 1 in ref. [44] appears to bear out this conclusion for N_{eff} . Moreover, had we introduced a flavor asymmetry in the interaction matrix, i.e., $g_{ee} \neq g_{\mu\mu}$, then we might expect some flavors of neutrinos to stay in self-equilibrium and others to evolve in an out-of-equilibrium fashion. Figure 1 shows there is little difference between these two kinds of distributions, so again we expect little effect on parameters. What may be different would be the case where there exists lepton asymmetries. If the self-interacting Lagrangian is indeed flavor biased, then lepton numbers can be different for different flavors, and oscillations would play a dominant effect during BBN [54–56]. Furthermore, the flavor-asymmetric scenario could have severe repercussions on neutrino free-streaming during atomic recombination, if the neutrino gas is only partially self-coupled. Such a scenario requires a calculation with vacuum neutrino oscillations, but we can give a qualitative description here. In the standard cosmology, free-streaming neutrinos cause a phase shift in the CMB acoustic peaks [57, 58]. The $SI\nu$ gas eliminates that phase shift and utilizes extra dark radiation to remedy this particular temperature power-spectrum defect. If not all the neutrinos were to be self-coupled, then the free-streaming neutrino component would induce a small phase shift, and the amount of dark radiation would necessarily be smaller. At the current epoch, the effect would be to increase the Hubble parameter only slightly.

In addition to all flavors being self-interacting, $SI\nu$ scenarios which remedy the Hubble parameter tension also stipulate the anti-neutrinos to be self-interacting. If the interacting Lagrangian in eq. (1.1) is not CP-symmetric, then models which use $SI\nu$ to resolve cosmological tensions will also confront the same problems as the flavor-asymmetric models discussed above. From the perspective of BBN, if anti-neutrinos do not remain in a self-equilibrium, then the anti-neutrino spectra would follow the dashed lines in figure 1 while the neutrinos followed the solid line. Again, we do not expect the asymmetry to cause significant changes in cosmological parameters related to BBN. With the introduction of a lepton number, we still would expect equal lepton numbers in all flavors as self-interactions will change the flavor content in the neutrino sector and standard model interactions will then equilibrate the numbers of neutrinos and anti-neutrinos such that all have identical chemical potentials.

In our analyses of neutrino-anti-neutrino asymmetry, we have always made the assumption that the net lepton number (i.e., the sum of the three flavor lepton numbers) cannot change. For the Lagrangian in eq. (1.1), this is certainly true. We could alter the Lagrangian to include right-handed neutrinos, with an operator such as $\overline{\nu_R}\nu_L\varphi$. For Majorana character, left-handed states could undergo spin-flips to the right-handed states at the same rate as the processes which equilibrate the neutrino/anti-neutrino seas. A lepton asymmetry cannot persist in such a scenario. If neutrinos are Dirac fermions, then the spin-flip populates the opposite helicity states. These states are inactive under the weak interaction, but would still have ramifications on BBN as they contribute to the radiation energy density and would raise $N_{\rm eff}$. The spin-flip interactions would have to freeze-out well before BBN [59] for a $SI\nu$ model with right-handed neutrinos to be viable. As a corollary, BBN would proceed without $SI\nu$ interactions but with the addition of dark radiation. Alternatively, if we were to consider vector mediators, then lepton number would not be conserved and we would expect a symmetric system. We do not anticipate any further implications for either BBN or photon decoupling if the mediator is a vector. Another possibility in the class of $SI\nu$ models is for a pseudoscalar mediator. In this scenario, neutrinos may recouple after weak decoupling [60]. Some late portion of recombination could transpire with equilibrium neutrino spectra, but BBN would occur with out-of-equilibrium distributions identical to the standard scenario.

Returning to the scalar-mediator scenario, we only considered the case when the mass of the mediator is much larger than BBN energy scales. If this were not the case, then it is possible for the mediator to be produced on shell, through reactions like $\nu + \nu \to \phi + \phi$, during BBN. As we take the self-interactions strong enough to ensure neutrino self-equilibrium throughout BBN, light mediators will continue to remain in equilibrium with the neutrino seas until the neutrinos decouple from themselves at late times. There are three ramifications of this. First, the φ -sea acts as a heat bath for neutrinos without conserving number. With a heat bath and strong coupling, the neutrino seas are in thermal and chemical equilibrium with temperature T_{ν} and vanishing η_{ν} . The evolution of T_{ν} and η_{ν} in eqs. (3.5) and (3.6) no longer apply, and we would have to construct an analog of eq. (2.9) for the ν - φ system. Second, if a φ -sea persists to times after weak decoupling, then there will be extra energy density in the ν - φ system which will become only neutrino and therefore increase the radiation energy density and $N_{\rm eff}$. This extra energy density is not dark radiation and will have ramifications on temperature power spectra [22]. Lastly, the energy in the φ -sea will heat the neutrinos to higher temperatures. If this occurs prior to helium formation, the higher neutrino temperature will cause a lower neutron-to-proton ratio and a smaller amount of helium.

Our final retrospection on the SI ν framework presented in this paper, is if we remove the stipulation that the neutrinos stayed in self-equilibrium throughout BBN. This is a class of models where $G_{\rm eff} \sim G_F$ and would not be able to alleviate the Hubble tension. As the self-interactions only reshuffle neutrino energy density, we would expect changes to BBN observables to be somewhere between the standard and full SI ν scenarios. In this case, we would not expect significant changes in $\{N_{\rm eff}, Y_{\rm P}, {\rm D/H}\}$. The more interesting scenario would be for the case of mediators with masses low enough to have non-zero densities during BBN. If the self-interactions freeze-out prior to or during BBN, the population of φ may still be present and decay into high-energy neutrinos. Such a decay is necessarily an out-of-equilibrium process and would require a transport calculation. If this decay occurs during weak decoupling, there exists the possibility that energy and entropy flow from the neutrino seas into the electromagnetic plasma, opposite of the direction in standard weak decoupling. The abundances, especially D/H, are sensitive to this entropy flow. Given the precision on measuring D/H, BBN has the potential of putting stricter limits for the "weak-self-interacting" case than the stronger case considered in this work.

There can be other, non-cosmology constraints on some self-interacting sterile neutrino models. Such models with low enough scalar mass m_{φ} and utilizing Majorana neutrinos can produce a unique neutrino-less double beta decay signature. This is where the double beta decay nuclear mass difference is shared among two electrons and an undetected scalar [61]. This distinctive phase space signature has allowed Majoron-like models [17–19] with effective couplings $g > 10^{-3}$ [62] to be constrained. Future tonne-scale double beta decay detectors will have higher sensitivity and therefore likely will be able to extend these constraints. Finally, the Z^0 -width measurement obviously provides a stringent limit on the triplet versions but not the singlet versions of the Majoron-like models discussed above. There can be other such constraints, for example on four-neutrino couplings [63].

Neutrino physics can play a significant, even dominant role in the dynamics, evolution, and nucleosynthesis in some compact object environments. These include, for example, core collapse supernovae and binary neutron star mergers. Not surprisingly, BSM neutrino self-interactions may have dramatic effects in these venues. These effects could lead to constraints which can complement those derived from the early universe considerations discussed in this work. However, the origin of some of the potentially constrainable compact object effects is rooted in the same self-equilibration and flavor changing physics that affects weak decoupling

and BBN in the early universe. When it comes to neutrino self-interactions and flavor, the key difference between compact objects and the early universe is the very low entropy per baryon in the former venue. For example, the collapsing cores of supernovae are characterized by low entropy and highly degenerate electron lepton number carried by seas of electrons and electron neutrinos. When the neutrinos become trapped by coherent neutral current scattering on heavy nuclei, self-interactions can do two things: (1) effect rapid self-equilibration among the neutrinos, very much like the self-equilibration in the early universe discussed above: and (2) rapidly re-distribute the degenerate electron lepton number among all three neutrino flavors. Electron neutrinos can be converted to μ and τ species, opening phase space for electron capture, $e^- + p \rightarrow n + \nu_e$. Very quickly the electron lepton number residing in the degenerate sea of electrons is redistributed and entropy is generated. This can result in dramatic alteration of the physics of collapse [3, 64]. Moreover, after core bounce, the neutrinos can be "cooled" by adiabatic expansion of the strongly self-coupled neutrino gas. This could lead to a constraint if neutrino energies are reduced below the thresholds for the IMB [65] and Kamiokande II [66] experiments which detected the neutrino burst from supernova SN1987a [67].

In closing, we mention the importance of deuterium in BBN constraints. Although the topic of this work is $SI\nu$, our analysis applies to other BSM scenarios. Cosmological models which posit extra radiation energy density during BBN [68-71] necessarily change the abundances. In particular, helium and deuterium increase if that energy density is dark radiation, i.e., $\delta_{\rm dr} > 0$. This can be remedied using a positive lepton number, as both $Y_{\rm P}$ and D/H decrease, while $N_{\rm eff}$ and other neutrino cosmology parameters (i.e., the sum of the light neutrino masses) are little changed by modest values of L_{ν}^{\star} ($N_{\rm eff}$ and the abundances scale differently for large values of L_{ν}^{\star} [72]). However, the results of sections 4 and 5 show that the two abundances do not have identical scaling relations if $\delta_{\rm dr}$ and L_{ν}^{\star} are to be used in concert. In other words, dark radiation and lepton asymmetry cannot together assuage tensions in abundances. Given the precision in measuring the primordial D/H observable, changes of even a few percent could cause a strong tension. The situation would be even worse with precise measurements of ³He and ⁷Li, as the sign of the relative abundance changes is different compared to Y_P and D/H. At this point, other physical mechanisms would need to be invoked to mitigate internal BBN inconsistencies. Returning to the $SI\nu$ scenario, picking a mass of the φ mediator for neutrino entropy creation during BBN could change Y_P and D/H such that the two scaling relationships are identical when dark radiation is included. Such a requirement on $SI\nu$ — or any other BSM scenario which must reconcile Y_P and D/H with $N_{\rm eff}$ — will narrowly constrict the available parameter space.

Acknowledgments

We thank Luke Johns, Amol Patwardhan, André de Gouvêa, Yue Zhang, Walter Tangarife, and Julien Froustey for useful discussions. This research was conducted through the Network for Neutrinos, Nuclear Astrophysics and Symmetries collaboration and is supported by National Science Foundation, grant PHY-1630782, and Heising-Simons Foundation, grant 2017-228. We also acknowledge NSF grants PHY-1614864 and PHY-1914242 at University of California San Diego. This research used resources provided by the Los Alamos National Laboratory Institutional Computing Program, which is supported by the U.S. Department of Energy National Nuclear Security Administration under Contract No. 89233218CNA000001. We thank the referee for their helpful comments.

References

- [1] Particle Data Group, Review of Particle Physics, Phys. Rev. D 98 (2018) 030001 [INSPIRE].
- [2] G. Raffelt and J. Silk, Light neutrinos as cold dark matter, Phys. Lett. B 192 (1987) 65
 [INSPIRE].
- [3] G.M. Fuller, R. Mayle and J.R. Wilson, *The Majoron model and stellar collapse*, *Astrophys. J.* **332** (1988) 826 [INSPIRE].
- [4] B. Dasgupta and J. Kopp, Cosmologically Safe eV-Scale Sterile Neutrinos and Improved Dark Matter Structure, Phys. Rev. Lett. 112 (2014) 031803 [arXiv:1310.6337] [INSPIRE].
- [5] J.F. Cherry, A. Friedland and I.M. Shoemaker, Neutrino Portal Dark Matter: From Dwarf Galaxies to IceCube, arXiv:1411.1071 [INSPIRE].
- [6] N. Saviano, A. Mirizzi, O. Pisanti, P.D. Serpico, G. Mangano and G. Miele, Multi-momentum and multi-flavour active-sterile neutrino oscillations in the early universe: role of neutrino asymmetries and effects on nucleosynthesis, Phys. Rev. D 87 (2013) 073006 [arXiv:1302.1200] [INSPIRE].
- [7] F. Forastieri, M. Lattanzi, G. Mangano, A. Mirizzi, P. Natoli and N. Saviano, Cosmic microwave background constraints on secret interactions among sterile neutrinos, JCAP 07 (2017) 038 [arXiv:1704.00626] [INSPIRE].
- [8] L. Johns and G.M. Fuller, Self-interacting sterile neutrino dark matter: the heavy-mediator case, Phys. Rev. D 100 (2019) 023533 [arXiv:1903.08296] [INSPIRE].
- [9] A. De Gouvêa, M. Sen, W. Tangarife and Y. Zhang, Dodelson-Widrow Mechanism in the Presence of Self-Interacting Neutrinos, Phys. Rev. Lett. 124 (2020) 081802
 [arXiv:1910.04901] [INSPIRE].
- [10] F.-Y. Cyr-Racine and K. Sigurdson, Limits on Neutrino-Neutrino Scattering in the Early Universe, Phys. Rev. D 90 (2014) 123533 [arXiv:1306.1536] [INSPIRE].
- [11] C.D. Kreisch, F.-Y. Cyr-Racine and O. Doré, *The Neutrino Puzzle: Anomalies, Interactions and Cosmological Tensions*, arXiv:1902.00534 [INSPIRE].
- [12] G. Barenboim, P.B. Denton and I.M. Oldengott, Constraints on inflation with an extended neutrino sector, Phys. Rev. **D** 99 (2019) 083515 [arXiv:1903.02036] [INSPIRE].
- [13] K.S. Babu, G. Chauhan and P.S. Bhupal Dev, Neutrino Non-Standard Interactions via Light Scalars in the Earth, Sun, Supernovae and the Early Universe, Phys. Rev. **D** 101 (2020) 095029 [arXiv:1912.13488] [INSPIRE].
- [14] M. Blennow, A. Mirizzi and P.D. Serpico, Nonstandard neutrino-neutrino refractive effects in dense neutrino gases, Phys. Rev. D 78 (2008) 113004 [arXiv:0810.2297] [INSPIRE].
- [15] A. Das, A. Dighe and M. Sen, New effects of non-standard self-interactions of neutrinos in a supernova, JCAP 05 (2017) 051 [arXiv:1705.00468] [INSPIRE].
- [16] A. Dighe and M. Sen, Nonstandard neutrino self-interactions in a supernova and fast flavor conversions, Phys. Rev. **D** 97 (2018) 043011 [arXiv:1709.06858] [INSPIRE].
- [17] G.B. Gelmini and M. Roncadelli, Left-Handed Neutrino Mass Scale and Spontaneously Broken Lepton Number, Phys. Lett. B 99 (1981) 411 [INSPIRE].
- [18] H.M. Georgi, S.L. Glashow and S. Nussinov, Unconventional Model of Neutrino Masses, Nucl. Phys. B 193 (1981) 297 [INSPIRE].
- [19] B. Grinstein, J. Preskill and M.B. Wise, Neutrino Masses and Family Symmetry, Phys. Lett. B 159 (1985) 57 [INSPIRE].
- [20] J.M. Berryman, A. De Gouvêa, K.J. Kelly and Y. Zhang, Lepton-Number-Charged Scalars and Neutrino Beamstrahlung, Phys. Rev. D 97 (2018) 075030 [arXiv:1802.00009] [INSPIRE].

- [21] K.J. Kelly and Y. Zhang, Mononeutrino at DUNE: New Signals from Neutrinophilic Thermal Dark Matter, Phys. Rev. D 99 (2019) 055034 [arXiv:1901.01259] [INSPIRE].
- [22] N. Blinov, K.J. Kelly, G.Z. Krnjaic and S.D. McDermott, Constraining the Self-Interacting Neutrino Interpretation of the Hubble Tension, Phys. Rev. Lett. 123 (2019) 191102 [arXiv:1905.02727] [INSPIRE].
- [23] E.W. Kolb and M.S. Turner, The Early Universe, Addison-Wesley Publishing Co. (1990).
- [24] A.G. Riess, S. Casertano, W. Yuan, L.M. Macri and D. Scolnic, Large Magellanic Cloud Cepheid Standards Provide a 1% Foundation for the Determination of the Hubble Constant and Stronger Evidence for Physics beyond ΛCDM, Astrophys. J. 876 (2019) 85 [arXiv:1903.07603] [INSPIRE].
- [25] P.S. Pasquini and O.L.G. Peres, *Bounds on Neutrino-Scalar Yukawa Coupling*, *Phys. Rev.* **D** 93 (2016) 053007 [*Erratum ibid.* **D 93** (2016) 079902] [arXiv:1511.01811] [INSPIRE].
- [26] J.M. Berryman, A. De Gouvêa, K.J. Kelly and Y. Zhang, Lepton-Number-Charged Scalars and Neutrino Beamstrahlung, Phys. Rev. D 97 (2018) 075030 [arXiv:1802.00009] [INSPIRE].
- [27] R.V. Wagoner, W.A. Fowler and F. Hoyle, On the Synthesis of elements at very high temperatures, Astrophys. J. 148 (1967) 3 [INSPIRE].
- [28] A.D. Dolgov, Neutrinos in cosmology, Phys. Rept. 370 (2002) 333 [hep-ph/0202122] [INSPIRE].
- [29] S. Weinberg, Cosmology, Oxford University Press (2008).
- [30] R.H. Cyburt, B.D. Fields, K.A. Olive and T.-H. Yeh, Big Bang Nucleosynthesis: 2015, Rev. Mod. Phys. 88 (2016) 015004 [arXiv:1505.01076] [INSPIRE].
- [31] E. Grohs, G.M. Fuller, C.T. Kishimoto, M.W. Paris and A. Vlasenko, Neutrino energy transport in weak decoupling and big bang nucleosynthesis, Phys. Rev. **D** 93 (2016) 083522 [arXiv:1512.02205] [INSPIRE].
- [32] L. Kawano, Let's go: Early universe II. Primordial nucleosynthesis. The computer way, FERMILAB-PUB-92-004-A (1992) [N-92-25163] [INSPIRE].
- [33] A.R. Howe, E. Grohs and F.C. Adams, Nuclear Processes in Other Universes: Varying the Strength of the Weak Force, Phys. Rev. D 98 (2018) 063014 [arXiv:1809.05128] [INSPIRE].
- [34] E. Grohs and G.M. Fuller, Insights into neutrino decoupling gleaned from considerations of the role of electron mass, Nucl. Phys. B 923 (2017) 222 [arXiv:1706.03391] [INSPIRE].
- [35] A.F. Heckler, Astrophysical applications of quantum corrections to the equation of state of a plasma, Phys. Rev. D 49 (1994) 611 [INSPIRE].
- [36] N. Fornengo, C.W. Kim and J. Song, Finite temperature effects on the neutrino decoupling in the early universe, Phys. Rev. **D** 56 (1997) 5123 [hep-ph/9702324] [INSPIRE].
- [37] J.J. Bennett, G. Buldgen, M. Drewes and Y.Y.Y. Wong, Towards a precision calculation of the effective number of neutrinos N_{eff} in the Standard Model I: The QED equation of state, JCAP 03 (2020) 003 [arXiv:1911.04504] [INSPIRE].
- [38] E. Grohs and G.M. Fuller, The surprising influence of late charged current weak interactions on Big Bang Nucleosynthesis, Nucl. Phys. B 911 (2016) 955 [arXiv:1607.02797] [INSPIRE].
- [39] O. Pisanti et al., PArthENoPE: Public Algorithm Evaluating the Nucleosynthesis of Primordial Elements, Comput. Phys. Commun. 178 (2008) 956 [arXiv:0705.0290] [INSPIRE].
- [40] A. Arbey, AlterBBN: A program for calculating the BBN abundances of the elements in alternative cosmologies, Comput. Phys. Commun. 183 (2012) 1822 [arXiv:1106.1363] [INSPIRE].
- [41] C. Pitrou, A. Coc, J.-P. Uzan and E. Vangioni, Precision big bang nucleosynthesis with improved Helium-4 predictions, Phys. Rept. **754** (2018) 1 [arXiv:1801.08023] [INSPIRE].

- [42] E. Grohs, G.M. Fuller, C.T. Kishimoto and M.W. Paris, Probing neutrino physics with a self-consistent treatment of the weak decoupling, nucleosynthesis and photon decoupling epochs, JCAP 05 (2015) 017 [arXiv:1502.02718] [INSPIRE].
- [43] Planck collaboration, *Planck 2018 results. VI. Cosmological parameters*, arXiv:1807.06209 [INSPIRE].
- [44] M. Escudero Abenza, Precision Early Universe Thermodynamics made simple: N_{eff} and Neutrino Decoupling in the Standard Model and beyond, JCAP 05 (2020) 048 [arXiv:2001.04466] [INSPIRE].
- [45] E. Aver, K.A. Olive, R.L. Porter and E.D. Skillman, *The primordial helium abundance from updated emissivities*, *JCAP* 11 (2013) 017 [arXiv:1309.0047] [INSPIRE].
- [46] R.J. Cooke, M. Pettini and C.C. Steidel, One Percent Determination of the Primordial Deuterium Abundance, Astrophys. J. 855 (2018) 102 [arXiv:1710.11129] [INSPIRE].
- [47] J. Froustey and C. Pitrou, *Incomplete neutrino decoupling effect on big bang nucleosynthesis*, *Phys. Rev.* **D 101** (2020) 043524 [arXiv:1912.09378] [INSPIRE].
- [48] S. Mukohyama, Brane world solutions, standard cosmology and dark radiation, Phys. Lett. B 473 (2000) 241 [hep-th/9911165] [INSPIRE].
- [49] K. Abazajian et al., CMB-S4 Decadal Survey APC White Paper, Bull. Am. Astron. Soc. 51 (2019) 209 [https://doi.org/10.2172/1556957] [arXiv:1908.01062] [INSPIRE].
- [50] S.H. Hansen, G. Mangano, A. Melchiorri, G. Miele and O. Pisanti, Constraining neutrino physics with BBN and CMBR, Phys. Rev. D 65 (2002) 023511 [astro-ph/0105385] [INSPIRE].
- [51] J. Hamann, J. Lesgourgues and G. Mangano, *Using BBN in cosmological parameter extraction from CMB: A Forecast for PLANCK*, *JCAP* **03** (2008) 004 [arXiv:0712.2826] [INSPIRE].
- [52] J.P. Kneller and G. Steigman, BBN for pedestrians, New J. Phys. 6 (2004) 117 [astro-ph/0406320] [INSPIRE].
- [53] E. Grohs, G.M. Fuller, C.T. Kishimoto and M.W. Paris, Lepton asymmetry, neutrino spectral distortions and big bang nucleosynthesis, Phys. Rev. D 95 (2017) 063503 [arXiv:1612.01986] [INSPIRE].
- [54] A.D. Dolgov, S.H. Hansen, S. Pastor, S.T. Petcov, G.G. Raffelt and D.V. Semikoz, Cosmological bounds on neutrino degeneracy improved by flavor oscillations, Nucl. Phys. B 632 (2002) 363 [hep-ph/0201287] [INSPIRE].
- [55] E. Castorina et al., Cosmological lepton asymmetry with a nonzero mixing angle θ_{13} , Phys. Rev. D 86 (2012) 023517 [arXiv:1204.2510] [INSPIRE].
- [56] L. Johns, M. Mina, V. Cirigliano, M.W. Paris and G.M. Fuller, Neutrino flavor transformation in the lepton-asymmetric universe, Phys. Rev. D 94 (2016) 083505 [arXiv:1608.01336] [INSPIRE].
- [57] S. Bashinsky and U. Seljak, Neutrino perturbations in CMB anisotropy and matter clustering, Phys. Rev. D 69 (2004) 083002 [astro-ph/0310198] [INSPIRE].
- [58] B. Follin, L. Knox, M. Millea and Z. Pan, First Detection of the Acoustic Oscillation Phase Shift Expected from the Cosmic Neutrino Background, Phys. Rev. Lett. 115 (2015) 091301 [arXiv:1503.07863] [INSPIRE].
- [59] CMB-S4 collaboration, CMB-S4 Science Book, First Edition, arXiv:1610.02743 [INSPIRE].
- [60] M. Archidiacono and S. Hannestad, *Updated constraints on non-standard neutrino interactions* from Planck, JCAP **07** (2014) 046 [arXiv:1311.3873] [INSPIRE].
- [61] S.R. Elliott, A.A. Hahn and M.K. Moe, Direct Evidence for Two Neutrino Double Beta Decay in ⁸²Se, Phys. Rev. Lett. **59** (1987) 2020 [INSPIRE].

- [62] T. Brune and H. Päs, Massive Majorons and constraints on the Majoron-neutrino coupling, Phys. Rev. **D** 99 (2019) 096005 [arXiv:1808.08158] [INSPIRE].
- [63] K.M. Belotsky, A.L. Sudarikov and M.Y. Khlopov, Constraint on anomalous 4ν interaction, Phys. Atom. Nucl. **64** (2001) 1637 [INSPIRE].
- [64] R.V. Konoplich and M.Y. Khlopov, Constraints on triplet Majoron model due to observations of neutrinos from stellar collapse, Sov. J. Nucl. Phys. 47 (1988) 565 [INSPIRE].
- [65] R.M. Bionta et al., Observation of a Neutrino Burst in Coincidence with Supernova SN 1987a in the Large Magellanic Cloud, Phys. Rev. Lett. 58 (1987) 1494 [INSPIRE].
- [66] Kamiokande-II collaboration, Observation of a Neutrino Burst from the Supernova SN 1987a, Phys. Rev. Lett. 58 (1987) 1490 [Inspire].
- [67] S. Shalgar, I. Tamborra and M. Bustamante, Core-collapse supernovae stymie secret neutrino interactions, arXiv:1912.09115 [INSPIRE].
- [68] M. Wyman, D.H. Rudd, R.A. Vanderveld and W. Hu, Neutrinos Help Reconcile Planck Measurements with the Local Universe, Phys. Rev. Lett. 112 (2014) 051302 [arXiv:1307.7715] [INSPIRE].
- [69] A.V. Patwardhan and G.M. Fuller, Late-time vacuum phase transitions: Connecting sub-eV scale physics with cosmological structure formation, Phys. Rev. **D** 90 (2014) 063009 [arXiv:1401.1923] [INSPIRE].
- [70] G.B. Gelmini, A. Kusenko and V. Takhistov, *Hints of Sterile Neutrinos in Recent Measurements of the Hubble Parameter*, arXiv:1906.10136 [INSPIRE].
- [71] V.E. Kuzmichev and V.V. Kuzmichev, Uncertainty principle in quantum mechanics with Newton's gravity, Eur. Phys. J. C 80 (2020) 248 [arXiv:1911.01176] [INSPIRE].
- [72] G. Mangano, G. Miele, S. Pastor, O. Pisanti and S. Sarikas, Constraining the cosmic radiation density due to lepton number with Big Bang Nucleosynthesis, JCAP 03 (2011) 035 [arXiv:1011.0916] [INSPIRE].